Inhibitory Actions of the Gamma-Aminobutyric Acid in Pediatric Sturge-Weber Syndrome

Roman Tyzio, PhD,[1] Ilgam Khalilov, PhD,[1] Alfonso Represa, MD, PhD,[1] Valerie Crepel, PhD,[1] Yuri Zilberter, PhD,[1] Sylvain Rheims, MD, PhD,[1] Laurent Anikstejn, PhD,[1] Rosa Cossart, PhD,[1] Romain Nardou,[1] Marat Mukhtarov, PhD,[1] Marat Minlebaev, MD, PhD,[1] Jérôme Epsztein, PhD,[1] Mathieu Milh, MD, PhD,[1] Helene Becq, PhD,[1] Isabel Jorquera,[1] Christine Bulteau, MD,[2] Martine Fohlen, MD,[2] Viviana Oliver, MD,[2] Olivier Dulac,[3] Georg Dorfmüller, MD,[2] Olivier Delalande, MD,[2] Yehezkel Ben-Ari, PhD,[1] and Roustem Khazipov, MD, PhD[1]

Objective: The mechanisms of epileptogenesis in Sturge-Weber syndrome (SWS) are unknown. We explored the properties of neurons from human pediatric SWS cortex *in vitro* and tested in particular whether gamma-aminobutyric acid (GABA) excites neurons in SWS cortex, as has been suggested for various types of epilepsies.

Methods: Patch-clamp and field potential recordings and dynamic biphoton imaging were used to analyze cortical tissue samples obtained from four 6- to 14-month-old pediatric SWS patients during surgery.

Results: Neurons in SWS cortex were characterized by a relatively depolarized resting membrane potential, as was estimated from cell-attached recordings of N-methyl-D-aspartate channels. Many cells spontaneously fired action potentials at a rate proportional to the level of neuronal depolarization. The reversal potential for GABA-activated currents, assessed by cell-attached single channel recordings, was close to the resting membrane potential. All spontaneously firing neurons recorded in cell-attached mode or imaged with biphoton microscopy were inhibited by GABA. Spontaneous epileptiform activity in the form of recurrent population bursts was suppressed by glutamate receptor antagonists, the GABA(A) receptor agonist isoguvacine, and the positive allosteric GABA(A) modulator diazepam. Blockade of GABA(A) receptors aggravated spontaneous epileptiform activity. The NKCC1 antagonist bumetanide had little effect on epileptiform activity.

Interpretation: SWS cortical neurons have a relatively depolarized resting membrane potential and spontaneously fire action potentials that may contribute to increased network excitability. In contrast to previous data depicting excitatory and proconvulsive actions of GABA in certain pediatric and adult epilepsies, GABA plays mainly an inhibitory and anticonvulsive role in SWS pediatric cortex.

Ann Neurol 2009;66:209–218

Epilepsy in infancy is often a catastrophic, life-threatening disorder.[1,2] The pathophysiological mechanisms of epileptogenesis in the immature brain nevertheless remain poorly understood.[3–5] Recently, the depolarizing and excitatory actions of gamma-aminobutyric acid (GABA) have been suggested to contribute to the greater excitability of the immature cortex.[4,6-11] Depolarizing GABA responses have been shown in dysplastic neurons from pediatric patients with cortical dysplasia[12] and in a population of subicular neurons in adult patients with temporal lobe epilepsy.[13] These findings suggest that depolarizing GABA is a common feature of developmental epilepsies. Here, we tested this hypothesis in the cortex of pediatric patients with Sturge-Weber syndrome (SWS).

SWS is a rare sporadic, neurocutaneous syndrome affecting the cephalic microvasculature. A decrease in cerebral blood flow within the cortical areas affected by the pial angiomatosis as well as decreased venous return, focal hypoxia, ischemia, and decreased neuronal metabolism are considered the main pathogenetic mechanisms of SWS.[14–17] Seizures are a common neurological symptom, most often appearing in SWS patients within the first year of life.[18–22] Surgical treatment to remove or disconnect the epileptic cortical region is the choice for about half of SWS patients.[23]

From [1]INMED-INSERM U901, Marseille; [2]Department of Pediatric Neurosurgery, Ophthalmological Fondation A, de Rothschild, A. de Rothschild, Paris; and [3]Neuropediatric Department, Necker-Enfants Malades University Hospital, Paris, France.

Address correspondence to Dr Khazipov, INMED-INSERM U901, 163 route de Luminy, Marseille 13273, France. E-mail: khazipov@inmed.univ-mrs.fr

Potential conflict of interest: Nothing to report.

Additional Supporting Information may be found in the online version of this article.

Received Jan 16, 2009, and in revised form Mar 18. Accepted for publication Mar 20, 2009. Published online in Wiley InterScience (www.interscience.wiley.com). DOI: 10.1002/ana.21711

Hemispheric disconnection using hemispherotomy techniques provides the highest success rate for seizure treatment in patients with severe epilepsy associated with a hemispheric SWS.[24] To understand the cellular and neuronal network mechanisms underlying epilepsy in pediatric SWS cortex, and in particular, to test the hypothesis that depolarizing GABA is a prominent feature of the pediatric epileptic SWS cortex, we examined cortical samples obtained during hemispherotomies from 4 SWS patients aged 6 to 14 months.

Materials and Methods

Patients

Informed consent for the use of postsurgical tissue for research purposes was obtained with a protocol approved by the institutional review board at the Rothschild Foundation.

Experimental System

Neocortical slices (350–500μm) were cut using the Vibratome (VT 1000E; Leica, Nussloch, Germany). Slices were kept in oxygenated (95% O_2/5% CO_2) artificial cerebrospinal fluid (ACSF) of the following composition (in mM): NaCl 126, KCl 3.5, $CaCl_2$ 2.0, $MgCl_2$ 1.3, $NaHCO_3$ 25, NaH_2PO_4 1.2, and glucose 11 (pH 7.4) at room temperature (20–22°C) at least 1 hour before use. For recordings, slices were placed into a conventional fully submerged chamber superfused with ACSF (30–32°C) at a rate of 2–3ml/min.

Electrophysiological Recordings and Data Analysis

Patch-clamp recordings from visually identified neuronal cells were performed using Axopatch 200A, 200B (Axon Instruments, Union City, CA) and EPC-9, EPC-10 (HEKA Elektronik, Lambrecht/Pfalz, Germany) amplifiers. Patch electrodes were made from borosilicate glass capillaries of 1.5mm outer diameter and 0.86mm inner diameter (GC150F-15, Clark Electromedical Instruments, Pangbourne, UK). For recordings of single GABA(A) channels, the patch pipette solution contained (in mM): NaCl 120, TEA-Cl 20, KCl 5, 4-aminopyridine 5, CaCl2 0.1, MgCl2 10, glucose 10, Hepes-NaOH 10 buffered to pH 7.2–7.3, and GABA (1–5μM) was added on the day of experiment from a 1mM frozen stock solution. GABA(A) driving force (DF_{GABA}) values were obtained from the reversal potential of currents through GABA(A) channels and were corrected for +2.1mV.[25] Membrane potential was estimated using cell-attached recordings of single N-methyl-D-aspartate (NMDA) channels as previously described.[26,27] For recordings of single NMDA channels, the pipette solution contained nominally Mg^{2+}-free ACSF with NMDA (10μM) and glycine (1μm). For whole-cell recordings, the patch pipette solution contained (in mM): potassium gluconate 135, NaCl 13, MgCl2 1, CaCl2 0.1, ethylene glycol tetraacetic acid 1, HEPES 10, pH 7.2. A picospritzer (General Valve Corporation, Fairfield, NJ) was used to puff-apply isoguvacine (10–100μM in ACSF) from a glass pipette at a distance of about 100μM from the soma in cell-attached recordings. The pressure was between 10 and 20kPa, and the duration of the puff varied from 50 to 200 milliseconds.

Extracellular field potentials were recorded using electrodes made from 50μm diameter tungsten wire. Signals were amplified using a custom-made amplifier (bandpass 0.1Hz–4kHz; ×1,000). For single action potential detection, records were filtered with a RC (single pole) high-pass filter at >200Hz. Recordings were digitized (10kHz) using a Digidata (Axon Instruments, Union City, CA) and analyzed with the Axon software package, Mini Analysis Program (Synaptosoft, Decatur, GA), and Origin 5.0 (Microcal Software, Northampton, MA). Group measures are expressed as means ± standard error (SE); error bars also indicate SE. The statistical significance of differences was assessed with the Student t test. The level of significance was set at $p < 0.05$.

Two-Photon Imaging

For calcium indicator loading, slices were incubated in a small chamber containing 2ml of oxygenated ACSF with 25μl of 1mM Fura2-AM solution (Invitrogen, Carlsbad, CA; in 100% dimethylsulfoxide) for 25 minutes at 35°C. Two-photon imaging was performed as described previously.[28] Briefly, experiments were performed at 32°C in oxygenated ACSF using a multibeam two-photon laser scanning system (Chameleon Ti:Sapphire laser, Coherent, Inc., Santa Clara, CA; and TriM scanhead, LaVision BioTec, Bielefeld, Germany) coupled to an Olympus (Center Valley, PA) BX51W1 microscope. The excitation wavelength was 780μm. Imaging was performed using a 20× 0.95NA objective (XLUMPLFL, Olympus) and a charge-coupled device camera (Imager Intense, LaVision, Goettingen, Germany) with an acquistion rate of ~100ms/frame. Image processing was performed using ImageJ 1.37 (National Institutes of Health, Bethesda, MD) and custom software in MATLAB (Mathworks, Natick, MA) described previously.[28] Cell contours were identified using a combination of automatic and visual detection routines. The calcium signals of each cell were the average fluorescence intensity inside each cell soma region of interest, measured as a function of time. Calcium events were manually identified, with automatic detection routines confirming events as local minima (typically <-2 standard deviations of the derivative of the signal). Analysis was performed with custom-made software in MATLAB (MathWorks) written by D. Aronov (Massachusetts Institute of Technology, Cambridge, MA).[28,29] Signal-processing algorithms of MiniAnalysis software (Synaptosoft) were used to detect the onsets and offsets (time of half-amplitude decay) of calcium signals within the traces of individual cells. Active cells are neurons exhibiting at least 1 calcium event within the period of recording. Calcium changes below 5% of the fractional change of fluorescence (DF/F) were discarded, because calibration of the imaging system showed that, on average, a single action potential will produce a fluorescence change always above this value.[28,29] Peak coactive network activity was quantified as the maximum percentage of cells exhibiting a calcium event at 1 time during a recording period.

Morphology

For each tissue specimen, 1 or 2 slices were fixed with paraformaldehyde (4% in phosphate-buffered saline) overnight and then embedded in agar and sliced again using a Vibratome (Vibratome Company, St. Louis, MO) (60μm) for Nissl staining. Visualization of biocytin-injected neurons was obtained with the avidin-biotin-peroxydase procedure (Vectastain Elite ABC; Vector Laboratories, Burlingame, CA) as described before,[25–27,30] and stained cells were reconstructed and analyzed using Neurolucida (MicroBrightField, Colchester, VT).

Results

Clinical Profile of Study Subjects

Tissue samples were obtained from 4 SWS patients undergoing surgical hemispherotomy, that is, a complete surgical disconnection of the affected cerebral hemisphere,[24] at the Division of Pediatric Neurosurgery, Rothschild Foundation between July 2005 and October 2007. The patient ages were 6, 9, 13, and 14 months (mean, 10.5 ± 1.8 months). The main patient characteristics are summarized in the Supplementary Table. All 4 infants had medically refractory epilepsy, hemiparesis or hemiplegia contralateral to the leptomeningeal angioma, associated with a developmental delay. All patients presented with a facial angioma ipsilateral to the leptomeningeal angioma, but 2 of them had more extensive cutaneous manifestations. Patient 2 presented hypertrophy of her right cheek and sparse cutaneous angioma of the left hemiface; patient 4 had bilateral facial angioma with hypertrophy of the left cheek and sparse cutaneous angioma on both shoulders and legs. Ocular manifestations were present in 2 infants: glaucoma (Patient 2) and megalocornea (Patient 3). Two infants (3 and 4) were treated with antiepileptic drugs before seizure onset. Patient 3 received vigabatrin from the age of 1 month until the age of 9 months, when it was stopped to avoid ocular side effects and was replaced by carbamazepine. Seizures appeared in the week following this drug transition.

Morphological Properties of Neurons in SWS Cortex

Histological analysis revealed variable alterations of cortical layering due to neuronal degeneration and loss. Many neurons contained perinuclear chromatin aggregates and nuclear condensation; pyknotic neurons were also frequently observed (Supplementary Fig 1). We also observed vessel alterations within the gray matter consisting mainly of irregular vascular dilatations and calcifications. All these findings are in agreement with previous descriptions of histopathological alterations of SWS cortex.[31-33] Twenty-three recorded neurons were visualized with biocytin staining. All were located in layers III to V (Supplementary Fig 2). Four cells were clearly identified as interneurons, with a multipolar or fusiform-bipolar shape; the remaining were pyramidal, but only 6 of them had clear projecting axons (i.e., those that reached the white matter). Dendritic and axonal arbors displayed variable degrees of complexity and length. However, most recorded neurons had small soma and dendrites that were tiny and poorly branched, reflecting a reduced degree of maturation. The total number of dendritic segments was 19 ± 5. The mean number of basal dendritic segments present was 15 ± 5, a third that of age-matched control deceased subjects with no neurological pathology (49 and 33 basal dendritic segments in layer IIIc and layer V, respectively) and even less than that observed in the 1-week-old newborn (20 and 31 segments in layer III and layer V, respectively).[34] Thus, neuronal maturation in SWS cortex is considerably impaired. Interestingly, cone-like growths were observed at the tip of some dendrites or axons in 3 SWS pyramidal neurons (Supplementary Fig 1F), suggesting that SWS neurons remain immature or undergo dynamic plasticity. In addition, a biocytin-filled structure resembling microglia was observed attached to 2 neurons from Patient 2, where it was attached to secondary or terminal dendrites (Supplementary Fig 1D, E). Microglia fused to apical dendrites have been observed in the cortex of virally infected rats,[35] where it was proposed that this type of fusion plays a role in phagocytic and immune responses to brain injury. This type of fusion would also allow the filling of satellite microglia by neuronal biocytin.

Resting Membrane Potential and Spontaneous Firing

We estimated the value of the membrane potential from cell-attached recordings of NMDA channels. The rationale of this approach is based on the fact that currents through NMDA channels reverse near 0mV,[36] and therefore in cell-attached recordings, NMDA currents should reverse their polarity at a pipette holding potential (V_p) equal to the resting membrane potential (E_m). Previous studies in neonatal rodents have shown that this noninvasive technique provides more reliable estimation of E_m than conventional whole-cell or perforated patch recordings, which are associated with an artifactual leak conductance that causes neuronal depolarization, which is particularly strong in small neurons.[25–27,30] Figure 1A shows examples of currents through NMDA channels recorded in the cell-attached configuration from a pyramidal cell at different values of V_p. Current-voltage relationships of currents through NMDA channels revealed a mean conductance of 60 ± 3pS (mean ± SE; n = 20 cells), comparable to values obtained from rodent neocortex[30] and granular cells from the adult human dentate of temporal lobe epilepsy (TLE) patients.[37] As estimated from the reversal of currents through NMDA channels, E_m values were highly variable, ranging from −43mV to −86mV, with a mean value of E_m −65 ± 3mV

(n=20; Fig 1B, C). These values are approximately 10 to 15mV more depolarized than those of young rodent neocortical neurons using a similar approach,[30] and than E_m values obtained in adult human neocortex from TLE patients with intracellular recordings (−79mV).[38] Many neurons in SWS cortex spontaneously fired action potentials, and the rate of spontaneous activity positively correlated with E_m ($R = 0.85$; n = 11 cells of 20; Fig 1D, E). However, 2 neurons with a strongly depolarized E_m of near −40mV did not fire action potentials. Subsequent whole-cell recordings showed that these cells were in a state of constant depolarization block (data not shown). Therefore, SWS neurons have a more depolarized E_m that will tend to augment excitability.

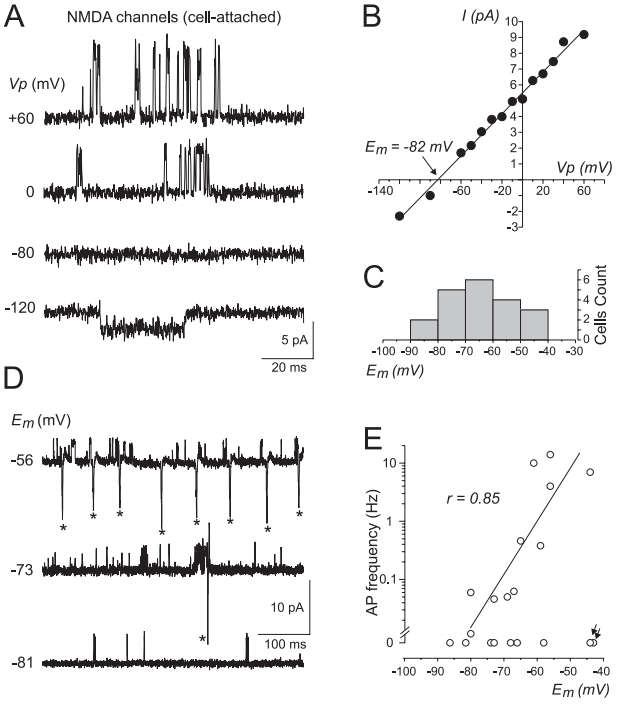

Fig 1. Membrane potential and spontaneous firing of Sturge-Weber syndrome (SWS) cortical neurons. (A) Cell-attached recordings of single N-methyl-D-aspartate (NMDA) channels from a pyramidal cell at various pipette potentials (V_P). Note that upward openings in cell-attached mode correspond to inward currents. (B) Corresponding current-voltage relationship of the currents through NMDA channels recorded in cell-attached mode. Note that currents through NMDA channels reverse at $V_P = -82mV$; assuming that NMDA receptor–mediated currents reverse at a membrane potential of 0mV, resting membrane potential (E_m) of this cell is −82mV. (C) Histogram plot of E_m values obtained in 20 cells in SWS cortex using cell-attached recordings of NMDA channels. (D) Examples of cell-attached recordings of NMDA channels and action potentials from 3 neurons ($V_P = 0mV$). E_m values that were deduced from the reversal potential of currents through NMDA channels are shown on the left. (E) Dependence of the action potential firing rate on E_m. Note that the frequency of spontaneous firing positively correlates with E_m except for 2 strongly depolarized cells (marked by arrows) that were in a state of depolarization block.

Effects of GABA

To characterize DF_{GABA}, we used cell-attached recordings of single GABA channels from the cell bodies of SWS neurons. This noninvasive recording technique has substantial advantages over other electrophysiological approaches to measure DF_{GABA}, because it affects neither E_{GABA} nor E_m,[39,40] nor is it compromised by space-clamp problems. Typical records of currents through GABA channels at different V_p are shown in Figure 2A. Currents through GABA(A) channels displayed slight outward rectification, and the current-voltage relationships were best fit with an exponential function. The tangent to the *I-V* curve at the reversal potential gave an estimate of the conductance of 15.1 ± 1.5pS (n = 15; Fig 2B).

In cell-attached recordings, the driving force acting on ions through GABA(A) channels is $-DF_{GABA} - V_p$. Therefore, DF_{GABA} equals $-V_p$ at the reversal potential of the currents through GABA(A) channels. As inferred from the *I-V* curves, DF_{GABA} varied within the range +16 to −6mV, with an average value of +3.1 ± 1.6mV (n = 15; Fig 2C). These DF_{GABA} values are close to those obtained in adult rodent neocortex and hippocampus, but are more negative than the values obtained in the neonatal rodents using cell-attached GABA(A) channel recordings[25,30,40] and gramicidin perforated patch recordings.[41–43] To estimate E_{GABA} we also measured E_m, using consequent cell-attached recordings of single NMDA channels from the same neurons (n = 10). Knowing DF_{GABA} and E_m, we further calculated E_{GABA} ($E_{GABA} = DF_{GABA} + E_m$). We found that E_{GABA} varies in the range between −80 to −39mV (mean, −64 ± 4mV; n = 10; Fig 2D). This is close to the average values of E_{GABA} obtained in the adult human neocortex of TLE patients with intracellular recordings, which are −68mV, for synaptic GABA(A) mediated responses and −69mV for responses evoked by the GABA(A) agonist.[38,44,45] Interestingly, there was a strong correlation between E_{GABA} and E_m; more depolarized neurons had more positive values of E_{GABA} (Fig 2E). These results differ from those observed in neurons from adult TLE subiculum, where despite the large variations in E_{GABA} and E_m, no correlation between these 2 parameters was observed.[46] To determine whether GABA exerts excitatory or inhibitory action on SWS cortical neurons, we also studied the effect of GABA(A) receptor activation on the frequency of action potentials in SWS neurons in cell-attached recordings. Using this technique, it has been previously shown that activation of GABA(A) receptors triggers action potentials in neonatal rodent cortical neurons, but inhibits neuronal firing

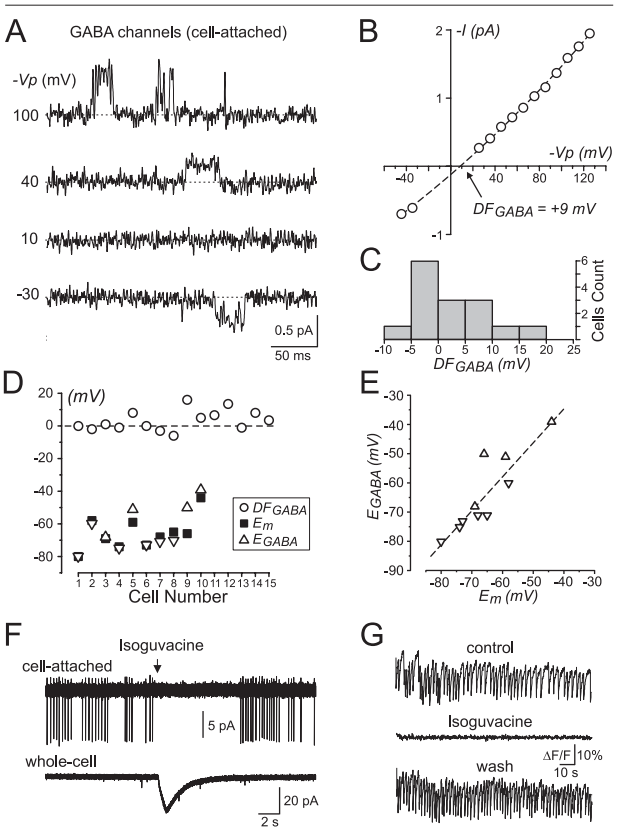

Fig 2. Gamma-aminobutyric acid (GABA) signaling in Sturge-Weber syndrome (SWS) cortical neurons. (A) Cell-attached recordings of single GABA(A) channels from a pyramidal cell at various pipette potentials (V_P). Note that both the currents and the V_P values are inverted. (B) Corresponding current-voltage relationship of the currents through GABA(A) channels recorded in cell-attached mode. Note that currents through GABA channels reverse at $V_P = +9mV$, corresponding to the driving force acting on ions passing through GABA(A) channels (DF_{GABA}). (C) Histogram plot of DF_{GABA} values obtained in 15 cells in SWS cortex using cell-attached recordings of GABA(A) channels. (D) Summary plot of DF_{GABA} and resting membrane potential (E_m) values obtained from cell-attached recordings of single GABA(A) and NMDA channels from each individual neuron, respectively. Resulting E_{GABA} was calculated as $E_{GABA} = DF_{GABA} + E_m$. Upward and downward triangles indicate depolarizing and hyperpolarizing GABA responses, respectively. (E) Dependence of E_{GABA} on E_m. Each point corresponds to an individual cell. Note that E_{GABA} strongly correlates with E_m. (F) The effect of a brief puff of the GABA(A) agonist isoguvacine on neuronal firing of a cell recorded in cell-attached mode. Note that isoguvacine transiently inhibits neuronal activity. Whole-cell response to the same puff of isoguvacine is shown below. (G) Biphoton imaging of intracellular calcium transients in spontaneously active SWS neuron. Note that activation of GABA(A) receptors with isoguvacine reversibly inhibits recurrent calcium transients.

in adolescent and adult cortex.[8,26,40,42,47] To activate GABA(A) receptors, the selective GABA(A) receptor agonist isoguvacine (100μM) was locally applied by brief pressure ejection. Isoguvacine failed to evoke action potentials in the silent neurons (those that did not fire spontaneous action potentials), and consistently inhibited neuronal firing in spontaneously active cells (n = 18; Fig 2F). To further assess the role of GABA signaling in slices obtained from SWS cortex, we used multibeam biphoton calcium imaging of cells loaded with the calcium indicator Fura2-AM. Many neurons displayed spontaneous calcium transients (Fig 2G) that have previously been shown to result from action potentials.[28,29] Bath application of isoguvacine (10μM for 1 minute) fully abolished these spontaneous calcium transients (control: 0.22 ± 0.06 second $^{-1}$ [n = 5 cells]); isoguvacine: 0s^{-1} [n = 5 cells]; wash: 0.18 ± 0.1s^{-1} [n = 4 cells]) confirming that GABA has an inhibitory action on neurons in SWS epileptic cortex.

Epileptic Activity

Despite severe clinical and electroencephalographic epileptic manifestations, only 4 slices from2 patients displayed synchronized epileptiform activity. This activity consisted of intermittent single or multiple population spikes associated with the bursts of multiple-unit activity (Fig 3A, B). Epileptiform events were typically observed in relatively small regions that did not exceed a few hundred microns in diameter. In these small, spontaneously epileptic zones, epileptiform events occurred simultaneously among multiple extracellular field potential recordings and were associated with large summated synaptic currents in concomitant whole-cell recordings. A large GABA-mediated component of the epileptic events was evident in whole-cell recordings with low-chloride–containing pipette solution at depolarized potentials (Fig 3C, D). Thus, spontaneous network activity recorded in SWS cortex had many features in common with the activity observed in adult epileptic neocortex and hippocampus.[13,46,48–52] Biphoton calcium imaging was also used to determine neuronal activity and network dynamics in SWS epileptic cortical slices. Fluorescence changes in the cell body of each imaged cell were analyzed in movies of spontaneous activity (field size: 430 × 380μm^2; 73 cells) to mark the onset and offset of individual calcium transients (Fig 4B). Calcium transients from all cells were then combined into raster plots showing the activity of each cell as a function of time (Fig 4C, D). Out of 73 imaged cells, we found 25 that were active, most of which exhibited multiple peaks of coactivity (Fig 4C, D) revealing a strongly coordinated network activity. This synchronous activity was driven by glutamatergic connections, as it was abolished by bath application of aminohydroxy methylisoxazole propionic acid and NMDA receptor antagonists (10μM 2,3-dihydro-6-nitro-7-sulfamoyl-benz quinoxaline and 40μM D-aminophosphonovalerate) in nearly all (96%)

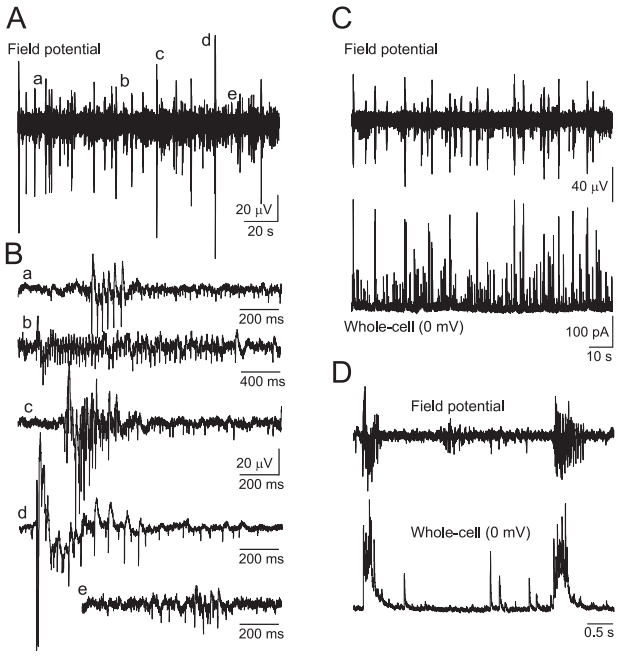

Fig 3. Spontaneous epileptiform activity in Sturge-Weber syndrome (SWS) cortical slices. (A) Field potential recordings from an SWS cortical slice (bandpass 1–5,000Hz). (B) Examples of spontaneous epileptiform population bursts from the trace shown on panel (A) on an expanded time scale. Note the variability of the epileptiform events, often associated with the population spikes and multiple unit activity. (C) Concomitant field potential and whole-cell recordings at 0mV holding potential with low-chloride–containing pipette solution so that the GABAergic currents are upwardly directed. (D) Two population bursts associated with large summated GABAergic synaptic currents are shown on an expanded time scale.

of imaged cells (Fig 4D). This further confirms that epileptiform activities in SWS cortex are driven by glutamatergic synapses, in keeping with electrophysiological data (Fig 4A) and previous findings in adult epileptic cortex (except that the activity in SWS cortex is more sensitive to NMDA receptor blockade[50]) and subiculum.[13]

We additionally addressed the role of GABA in the control of network activity in SWS cortex. It has previously been shown that blockade of GABA(A) receptors suppresses spontaneous recurrent network bursts observed in adult epileptic cortex[50–52] and in subiculum.[13] However, in SWS cortex, the GABA(A) receptor antagonist bicuculline (10μM) strongly increased the amplitude of spontaneous epileptiform events (Fig 5A). In contrast, application of the GABA(A) agonist isoguvacine (50μM) and of the positive GABA(A) allosteric modulator diazepam (10μM) suppressed epileptiform events (Fig 5B, C). We also tested the effect of bumetanide, a selective NKCC1 antagonist, which negatively shifts E_{GABA}[40,46,53,54] and exerts anticonvulsive effects in several animal epilepsy models[9,55,56] and in the slices from TLE patients.[46] However, in SWS cortex bumetanide (10μM) did not exert prominent effects on epileptiform activity (Fig 5D). Taken to-

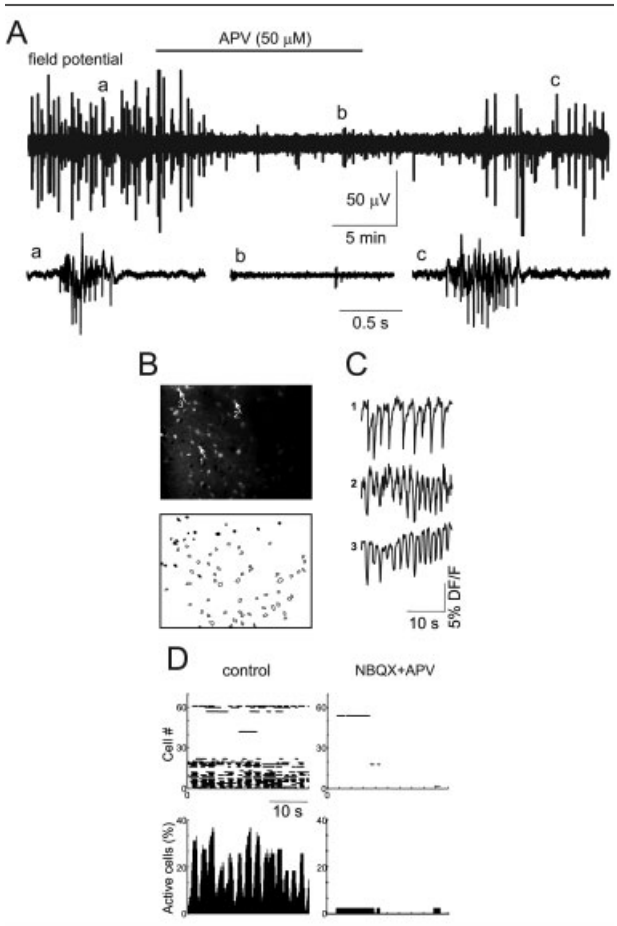

*Fig 4. Spontaneous epileptiform activity in Sturge-Weber syndrome (SWS) cortex is suppressed by glutamate receptor antagonists. (A) Field potential recordings of spontaneous epileptiform activity in an SWS cortical slice. Application of N-methyl-D-aspartate receptor antagonist D-aminophosphonovalerate (APV) completely suppressed the recurrent population bursts in a reversible manner. Below are shown examples of recordings on an expanded time scale. (B) A biphoton calcium fluorescence image of an SWS epileptic cortical slice (*top*). Detected contours of imaged cells (*bottom*); open contours indicate silent cells and black-filled contours indicate cells producing calcium transients. (C) Representative calcium transients recorded in 3 different cells (indicated by arrows in B). (D) Raster plots (*top*) of cell activity from the movie illustrated in (B); each row represents a single cell and each horizontal line the duration of detected calcium transients in the artificial cerebrospinal fluid (ACSF) condition (*left*) and in the presence of glutamatergic antagonists (10μm 2,3-dihydro-6-nitro-7-sulfamoyl-benz quinoxaline [NBQX] and 40μm APV,* right*). Histograms (*bottom*) showing the percentage of imaged cells that are detected as being active during the time of recording in the ACSF condition (*left*) and in the presence of glutamate receptor antagonists (10μm NBQX and 40μm D-APV,* right*). Time resolution: 100ms/frame.*

gether, these results suggest that GABA plays an inhibitory role in SWS epileptic pediatric cortex, in agreement with the inhibitory effects of GABA we found at the cellular level.

Discussion

The principal findings of the present study are as follows: 1) SWS pediatric epileptic cortex is characterized by neuronal degeneration and delayed maturation, as reflected by the relatively modest dendritic and axonal branching of cortical neurons and the presence of growth cones; 2) a significant number of SWS cortical neurons are depolarized and display spontaneous activity proportional to neuronal depolarization; and 3) GABA exerts inhibitory shunting action on SWS neurons and plays an anticonvulsive role in SWS cortex.

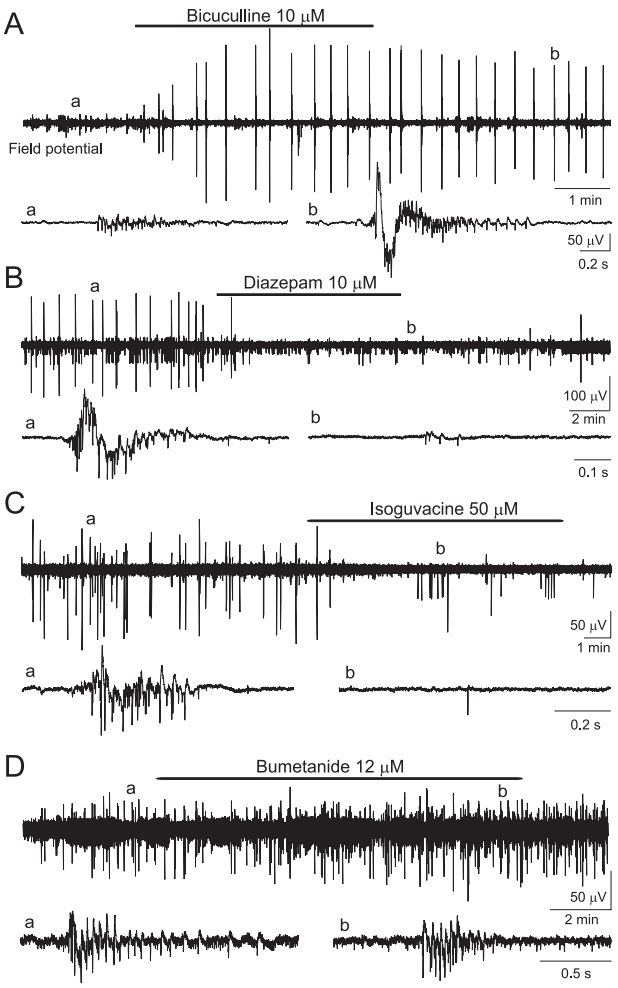

Fig 5. Inhibitory role of gamma-aminobutyric acid (GABA) in Sturge-Weber syndrome (SWS) pediatric cortex. Field potential recordings from SWS cortical slices display spontaneous epileptiform recurrent bursts of activity. (A) Blockade of GABA(A) receptors with bicuculline strongly enhances the amplitude of the epileptiform events. (B) The positive allosteric GABA(A) modulator diazepam completely suppresses the epileptiform activity; in the presence of diazepam, only nonorganized multiple unit activity remains. (C) The GABA(A) agonist isoguvacine also completely suppresses population bursts. (D) Blockade of NKCC1 with bumetanide does not significantly affect the spontaneous epileptiform activity.

Our finding of morphological signs of neuronal damage in SWS cortex is in agreement with the pathophysiological theory of reduced blood supply to the cortex in SWS due to an abnormal venous dilation that causes ischemic damage. Indeed, several morphological abnormalities observed in SWS neurons are characteristic of postischemic damage, mainly the presence of clear neuronal depletions that alter the normal cortical layering. That a significant number of cells are depolarized in SWS cortex is also more consistent with ischemic damage to the cortex than damage resulting from the epileptogenic process. Indeed, studies in human epileptic cortex have not revealed major abnormalities in resting membrane potential or electrogenesis[57] (although increased cellular excitability has been reported in pilocarpine and kainate models of epilepsy[58–61]; but reductions of pyramidal cell burst firing have also been noted[62]). Studies in postischemic rat cortex have, however, revealed depolarized values of E_m. For instance, in control and postischemic neocortical neurons values of E_m were −84mV and −78 mV, respectively.[63] Similar depolarized values of E_m have been also observed in CA3 pyramidal cells in the postischemic hippocampus (−72mV and −67mV in the control and postischemic hippocampus, respectively).[64] It has been suggested that a depolarized E_m contributes to enhanced excitability of postichemic cortex,[63,64] and this may also apply to SWS cortex. The mechanisms underlying neuronal depolarization are at present unknown. Although in situ this could reflect a diminished activity of energy-dependent mechanisms that maintain ionic gradients (including Na,K-ATPase) as a result of the compromised metabolic supply, our findings of depolarized E_m in conditions of normal oxygen and glucose supply in vitro support permanent, metabolic-supply–independent mechanisms. The mechanism causing a depolarized E_m in SWS cortex may involve alterations in the expression or function of many membrane proteins, including the HCN-channels,[61,65] A-type K^+ channels,[60] and the Na,K-ATPase.[66] Increased neuronal firing of neurons in SWS cortex, in proportion to the level of neuronal depolarization, should clearly contribute to increased excitability in the SWS cortex.

The central hypothesis tested in the present work was that depolarizing GABA is prevalent in SWS pediatric neocortex. Noninvasive measurements of DF_{GABA}, E_m, and E_{GABA} using cell-attached recordings revealed that E_{GABA} is close to E_m, and thus activation of GABA(A) receptors produces an isoelectric response, increasing membrane conductance without causing a significant change in membrane potential. Therefore,

GABA essentially inhibits SWS neurons via a shunting mechanism. In keeping with these observations, we found that activation of GABA(A) receptors inhibits neuronal firing and suppresses recurrent calcium transients in biphoton imaging experiments. The mechanism of this inhibition likely involves shunting of ongoing excitatory synaptic inputs and voltage-gated conductances involved in the generation of membrane potential oscillations that drive spontaneous firing. The results of our pharmacological analysis are also consistent with inhibitory and anticonvulsive roles for GABA at the network level. Indeed, blockade of GABA(A) receptors with bicuculline aggravated epileptiform discharges, whereas activation of GABA(A) receptors with isoguvacine and potentiation of endogenous GABA signaling with diazepam suppressed network activity. Bumetanide, whose antiepileptic action in certain developmental models has been linked to suppression of depolarizing GABA responses,[9,55,56] had no prominent effects on epileptiform activity in SWS cortex. Together, these results suggest that GABA exerts an inhibitory action, via a shunting mechanism, at both the cellular and network levels in pediatric SWS cortex. These results are interesting for 2 reasons. First, they indicate that the developmental switch in the action of GABA from excitatory to inhibitory occurs in human cortex before the time window of the present study (6–14 months). Second, it appears that the excitatory GABA phenotype observed as a part of some epileptogenic processes[11–13,46,67,68] is disease-model–specific, and is not present in the case of SWS. Clearly, further studies in younger patients and other epileptic diseases are required to determine when the developmental excitatory-to-inhibitory switch occurs in humans, and to determine the diseases associated with depolarizing GABA. Although we have not observed excitatory GABA responses in SWS neurons, E_{GABA} attained strongly depolarized absolute values in certain cells in an E_m-dependent manner, suggesting that cells with depolarized E_m have elevated intracellular chloride concentration. In keeping with this observation, using a clomeleon chloride sensor, elevated intracellular chloride has been reported following experimental ischemia in the cortical neurons.[69] A similar depolarizing shift of E_m and E_{GABA} without alteration in DF_{GABA} has also been recently observed in CA1 pyramidal cells of kainate-treated mice.[70] The similarity between E_m and E_{GABA} indicates that E_{GABA} is set at passive chloride equilibrium and that chloride transporters in SWS neurons are barely efficient. This is consistent with a downregulation of chloride cotransporters (notably KCC2) in TLE neurons.[9,55,56]

In the present study, we have shown that neocortical neurons in SWS cortex display a number of aberrant features that may result from chronic hypoxic/ischemic injury. These include depolarized membrane potentials along with increased spontaneous firing, which may contribute to increased excitability of SWS cortex. We have in addition provided evidence that GABA is inhibitory in the pediatric SWS cortex.

Financial support from the European Union (EC contract number LSH-CT-2006-037315 [EPICURE] FP6, thematic priority LIFESCIHEALTH to Y.B.A., A.R. and R.K.), INSERM, Agence Nationale de la Recherche to R.K., A.R., Fondation pour la Recherche Medicale to R.K., Ligue française contre l'epilepsie to M.M., and R.N., Rothschild/Inserm (to R.K.) and Necker/Inserm (to Y.B.A. and Y.Z.) "interface" programs is acknowledged.

References

1. Holmes GL. Effects of seizures on brain development: lessons from the laboratory. Pediatr Neurol 2005;33:1–11.
2. Ben Ari Y, Holmes GL. Effects of seizures on developmental processes in the immature brain. Lancet Neurol 2006;5: 1055–1063.
3. Cepeda C, Andre VM, Levine MS, et al. Epileptogenesis in pediatric cortical dysplasia: the dysmature cerebral developmental hypothesis. Epilepsy Behav 2006;9:219–235.
4. Ben Ari Y, Gaiarsa JL, Tyzio R, et al. GABA: A pioneer transmitter that excites immature neurons and generates primitive oscillations. Physiol Rev 2007;87:1215–1284.
5. Dube CM, Brewster AL, Richichi C, et al. Fever, febrile seizures and epilepsy. Trends Neurosci 2007;30:490–496.
6. Staley KJ. Wrong-way chloride transport: is it a treatable cause of some intractable seizures? Epilepsy Curr 2006;6:124–127.
7. Ben-Ari Y, Cherubini E, Corradetti R, et al. Giant synaptic potentials in immature rat CA3 hippocampal neurones. J Physiol 1989;416:303–325.
8. Khazipov R, Khalilov I, Tyzio R, et al. Developmental changes in GABAergic actions and seizure susceptibility in the rat hippocampus. Eur J Neurosci 2004;19:590–600.
9. Dzhala VI, Talos DM, Sdrulla DA, et al. NKCC1 transporter facilitates seizures in the developing brain. Nat Med 2005;11: 1205–1213.
10. Dzhala VI, Staley KJ. Excitatory actions of endogenously released GABA contribute to initiation of ictal epileptiform activity in the developing hippocampus. J Neurosci 2003;23: 1840–1846.
11. Khalilov I, Holmes GL, Ben Ari Y. In vitro formation of a secondary epileptogenic mirror focus by interhippocampal propagation of seizures. Nat Neurosci 2003;6:1079–1085.
12. Cepeda C, Andre VM, Wu N, et al. Immature neurons and GABA networks may contribute to epileptogenesis in pediatric cortical dysplasia. Epilepsia 2007;48(suppl 5):79–85.
13. Cohen I, Navarro V, Clemenceau S, et al. On the origin of interictal activity in human temporal lobe epilepsy in vitro. Science 2002;29
14. Comi AM. Advances in Sturge-Weber syndrome. Curr Opin Neurol 2006;19:124–128.
15. Chiron C, Raynaud C, Tzourio N, et al. Regional cerebral blood flow by SPECT imaging in Sturge-Weber disease: an aid for diagnosis. J Neurol Neurosurg Psychiatry 1989;52: 1402–1409.
16. Jordan LC, Wityk RJ, Dowling MM, et al. Transcranial Doppler ultrasound in children with Sturge-Weber syndrome. J Child Neurol 2008;23:137–143.
17. Namer IJ, Battaglia F, Hirsch E, et al. Subtraction ictal SPECT co-registered to MRI (SISCOM) in Sturge-Weber syndrome. Clin Nucl Med 2005;30:39–40.

18. Sujansky E, Conradi S. Sturge-Weber syndrome: age of onset of seizures and glaucoma and the prognosis for affected children. J Child Neurol 1995;10:49–58.
19. Kossoff EH, Hatfield LA, Ball KL, et al. Comorbidity of epilepsy and headache in patients with Sturge-Weber syndrome. J Child Neurol 2005;20:678–682.
20. Miyama S, Goto T. Leptomeningeal angiomatosis with infantile spasms. Pediatr Neurol 2004;31:353–356.
21. Sujansky E, Conradi S. Outcome of Sturge-Weber syndrome in 52 adults. Am J Med Genet 1995;57:35–45.
22. Ville D, Enjolras O, Chiron C, et al. Prophylactic antiepileptic treatment in Sturge-Weber disease. Seizure 2002;11:145–150.
23. Bourgeois M, Crimmins DW, de Oliveira RS, et al. Surgical treatment of epilepsy in Sturge-Weber syndrome in children. J Neurosurg 2007;106:20–28.
24. Bulteau C, Dorfmuller G, Fohlen M, et al. [Long-term outcome after hemispheric disconnection]. Neurochirurgie 2008; 54:358–361.
25. Tyzio R, Minlebaev M, Rheims S, et al. Postnatal changes in somatic gamma-aminobutyric acid signalling in the rat hippocampus. Eur J Neurosci 2008;27:2515–2528.
26. Leinekugel X, Medina I, Khalilov I, et al. Ca^{2+} oscillations mediated by the synergistic excitatory actions of $GABA_A$ and NMDA receptors in the neonatal hippocampus. Neuron 1997; 18:243–255.
27. Tyzio R, Ivanov A, Bernard C, et al. Membrane potential of CA3 hippocampal pyramidal cells during postnatal development. J Neurophysiol 2003;90:2964–2972.
28. Crepel V, Aronov D, Jorquera I, et al. A parturition-associated nonsynaptic coherent activity pattern in the developing hippocampus. Neuron 2007;54:105–120.
29. Goldin M, Epsztein J, Jorquera I, et al. Synaptic kainate receptors tune oriens-lacunosum moleculare interneurons to operate at theta frequency. J Neurosci 2007;27:9560–9572.
30. Rheims S, Minlebaev M, Ivanov A, et al. Excitatory GABA in rodent developing neocortex in vitro. J Neurophysiol 2008;100: 609–619.
31. Norman MG, Schoene WC. The ultrastructure of Sturge-Weber disease. Acta Neuropathol 1977;37:199–205.
32. Di Trapani G, Di Rocco C, Abbamondi AL, et al. Light microscopy and ultrastructural studies of Sturge-Weber disease. Childs Brain 1982;9:23–36.
33. Simonati A, Colamaria V, Bricolo A, et al. Microgyria associated with Sturge-Weber angiomatosis. Childs Nerv Syst 1994; 10:392–395.
34. Petanjek Z, Judas M, Kostovic I, et al. Lifespan alterations of basal dendritic trees of pyramidal neurons in the human prefrontal cortex: a layer-specific pattern. Cereb Cortex 2008;18: 915–929.
35. Ackman JB, Siddiqi F, Walikonis RS, et al. Fusion of microglia with pyramidal neurons after retroviral infection. J Neurosci 2006;26:11413–11422.
36. Nowak L, Bregestovski P, Ascher P, et al. Magnesium gates glutamate-activated channels in mouse central neurones. Nature 1984;307:462–465.
37. Lieberman DN, Mody I. Properties of single NMDA receptor channels in human dentate gyrus granule cells. J Physiol 1999; 518:55–70.
38. McCormick DA. GABA as an inhibitory neurotransmitter in human cerebral cortex. J Neurophysiol 1989;62:1018–1027.
39. Serafini R, Valeyev AY, Barker JL, et al. Depolarizing GABA-activated Cl^- channels in embryonic rat spinal and olfactory bulb cells. J Physiol 1995;488:371–386.
40. Tyzio R, Cossart R, Khalilov I, et al. Maternal oxytocin triggers a transient inhibitory switch in GABA signaling in the fetal brain during delivery. Science 2006;314:1788–1792.
41. Gulledge AT, Stuart GJ. Excitatory actions of GABA in the cortex. Neuron 2003;37:299–309.
42. Tyzio R, Holmes GL, Ben-Ari Y, et al. Timing of the developmental switch in GABA(A) mediated signalling from excitation to inhibition in CA3 rat hippocampus using gramicidin perforated patch and extracellular recordings. Epilepsia 2007;48: 96–105.
43. Owens DF, Boyce LH, Davis MB, et al. Excitatory GABA responses in embryonic and neonatal cortical slices demonstrated by gramicidin perforated-patch recordings and calcium imaging. J Neurosci 1996;16:6414–6423.
44. Avoli M, Olivier A. Electrophysiological properties and synaptic responses in the deep layers of the human epileptogenic neocortex in vitro. J Neurophysiol 1989;61:589–606.
45. Deisz RA. GABA(B) receptor-mediated effects in human and rat neocortical neurones in vitro. Neuropharmacology 1999;38: 1755–1766.
46. Huberfeld G, Wittner L, Clemenceau S, et al. Perturbed chloride homeostasis and GABAergic signaling in human temporal lobe epilepsy. J Neurosci 2007;27:9866–9873.
47. Khazipov R, Leinekugel X, Khalilov I, et al. Synchronization of GABAergic interneuronal network in CA3 subfield of neonatal rat hippocampal slices. J Physiol 1997;498:763–772.
48. Schwartzkroin PA, Knowles WD. Intracellular study of human epileptic cortex: in vitro maintenance of epileptiform activity? Science 1984;223:709–712.
49. Schwartzkroin PA, Haglund MM. Spontaneous rhythmic synchronous activity in epileptic human and normal monkey temporal lobe. Epilepsia 1986;27:523–533.
50. Kohling R, Lucke A, Straub H, et al. Spontaneous sharp waves in human neocortical slices excised from epileptic patients. Brain 1998;121:1073–1087.
51. Kohling R, Qu M, Zilles K, et al. Current-source-density profiles associated with sharp waves in human epileptic neocortical tissue. Neuroscience 1999;94:1039–1050.
52. Kohling R, Vreugdenhil M, Bracci E, et al. Ictal epileptiform activity is facilitated by hippocampal GABAA receptor-mediated oscillations. J Neurosci 2000;20:6820–6829.
53. Achilles K, Okabe A, Ikeda M, et al. Kinetic properties of Cl uptake mediated by Na+-dependent K+-2Cl cotransport in immature rat neocortical neurons. J Neurosci 2007;27: 8616–8627.
54. Yamada J, Okabe A, Toyoda H, et al. Cl− uptake promoting depolarizing GABA actions in immature rat neocortical neurones is mediated by NKCC1. J Physiol 2004;557:829–841.
55. Dzhala VI, Brumback AC, Staley KJ. Bumetanide enhances phenobarbital efficacy in a neonatal seizure model. Ann Neurol 2008;63:222–235.
56. Kilb W, Sinning A, Luhmann HJ. Model-specific effects of bumetanide on epileptiform activity in the in-vitro intact hippocampus of the newborn mouse. Neuropharmacology 2007; 53:524–533.
57. Avoli M, Louvel J, Pumain R, et al. Cellular and molecular mechanisms of epilepsy in the human brain. Prog Neurobiol 2005;77:166–200.
58. Sanabria ERC, Su HL, Yaari Y. Initiation of network bursts by Ca2+-dependent intrinsic bursting in the rat pilocarpine model of temporal lobe epilepsy. J Physiol 2001;532: 205–216.
59. Wellmer J, Su HL, Beck H, et al. Long-lasting modification of intrinsic discharge properties in subicular neurons following status epilepticus. Eur J Neurosci 2002;16:259–266.
60. Bernard C, Anderson A, Becker A, et al. Acquired dendritic channelopathy in temporal lobe epilepsy. Science 2004;305: 532–535.

61. Shah MM, Anderson AE, Leung V, et al. Seizure-induced plasticity of h channels in entorhinal cortical layer III pyramidal neurons. Neuron 2004;44:495–508.
62. Knopp A, Kivi A, Wozny C, et al. Cellular and network properties of the subiculum in the pilocarpine model of temporal lobe epilepsy. J Comp Neurol 2005;483:476–488.
63. Luhmann HJ, Mudrick-Donnon LA, Mittmann T, et al. Ischaemia-induced long-term hyperexcitability in rat neocortex. Eur J Neurosci 1995;7:180–191.
64. Congar P, Gaiarsa JL, Popovici T, et al. Permanent reduction of seizure threshold in post-ischemic CA3 pyramidal neurons. J Neurophysiol 2000;83:2040–2046.
65. Chen K, Aradi I, Thon N, et al. Persistently modified h-channels after complex febrile seizures convert the seizure-induced enhancement of inhibition to hyperexcitability. Nat Med 2001;7:331–337.
66. Ross ST, Soltesz I. Selective depolarization of interneurons in the early posttraumatic dentate gyrus: involvement of the Na(+)/K(+)-ATPase. J Neurophysiol 2000;83:2916–2930.
67. Khalilov I, Le Van QM, Gozlan H, et al. Epileptogenic actions of GABA and fast oscillations in the developing hippocampus. Neuron 2005;48:787–796.
68. de Guzman P, Inaba Y, Biagini G, et al. Subiculum network excitability is increased in a rodent model of temporal lobe epilepsy. Hippocampus 2006;16:843–860.
69. Pond BB, Berglund K, Kuner T, et al. The chloride transporter Na(+)-K(+)-Cl− cotransporter isoform-1 contributes to intracellular chloride increases after in vitro ischemia. J Neurosci 2006;26:1396–1406.
70. Le Duigou C, Bouilleret V, Miles R. Epileptiform activities in slices of hippocampus from mice after intra-hippocampal injection of kainic acid. J Physiol 2008;586:4891–4904.